applications to picture processing," *Inform. Sci.*, vol. 7, pp. 95–132, 1974.
[41] D. W. Murray, "Model-based recognition using 3D structure from motion," *Image Vision Comput.*, vol. 5, no. 2, pp. 85–90, 1987.
[42] W. A. Perkins, "A model-based vision system for industrial parts," *IEEE Trans. Comput.*, vol. C-27, no. 2, pp. 126–143, 1978.
[43] —, "Simplified model-based part locator," in *Proc. 5th Int. Conf. Pattern Recognition*, 1980, pp. 260–263.
[44] S. B. Pollard, J. Porrill, J. E. W. Mayhew, and J. P. Frisby, "Matching geometrical descriptions in three-space," *Image Vision Comput.*, vol. 5, no. 2, pp. 73–78, 1987.
[45] W. S. Rutkowski, "Recognition of occluded shapes using relaxation," *Comput. Graphics Image Processing*, vol. 19, pp. 111–128, 1982.
[46] W. S. Rutkowski, S. Peleg, and A. Rosenfeld, "Shape segmentation using relaxation," *IEEE Trans. Pattern Anal. Machine Intell.*, vol. 3, no. 4, pp. 368–375, 1981.
[47] J. T. Schwartz and M. Sharir, "Identification of partially obscured objects in two and three dimensions by matching noisy characteristic curves," *Int. J. Robotics Res.*, vol. 6, no. 2, pp. 29–44, 1987.
[48] J. Sklansky, "On the Hough technique for curve detection," *IEEE Trans. Comput.*, vol. C-27, pp. 923–926, 1978.
[49] G. Stockman and J. C. Esteva, "Use of geometrical constraints and clustering to determine 3D object pose," Dep. Comput. Sci., Michigan State Univ., Tech. Rep. TR84-002, 1984.
[50] J. L. Turney, T. N. Mudge, and R. A. Volz, "Recognizing partially occluded parts," *IEEE Trans. Pattern Anal. Machine Intell.*, vol. PAMI-7, no. 4, pp. 410–421, 1985.
[51] D. Waltz, "Understanding line drawings of scenes with shadows," in *The Psychology of Computer Vision*, P. Winston, Ed. New York: McGraw-Hill, 1975, pp. 19–91.

Range Image Segmentation Based on Differential Geometry: A Hybrid Approach

NAOKAZU YOKOYA AND MARTIN D. LEVINE

Abstract—**One of the most significant problems arising out of range data analysis is *image segmentation*. This correspondence describes a hybrid approach to the problem, where *hybrid* refers to a combination of both region- and edge-based considerations. The range image of 3-D objects is divided into *surface primitives* which are homogeneous in their intrinsic differential geometric properties and do not contain discontinuities in either depth or surface orientation. The method is based on the computation of partial derivatives which are obtained by a selective local biquadratic surface fit. Then by computing the Gaussian and mean curvatures, an initial region-based segmentation is obtained in the form of a curvature sign map. Two additional initial edge-based segmentations are also computed from the partial derivatives and depth values: *jump* and *roof edge* maps. The three image maps are then combined to produce the final segmentation. Experimental results were obtained for both synthetic and real range data of polyhedral and curved objects.**

Manuscript received September 25, 1987; revised November 2, 1988. Recommended for acceptance by C. R. Dyer. This work was supported in part by the Natural Sciences and Engineering Research Council of Canada under Grant G1840.

N. Yakoya is with the Electrotechnical Laboratory, Tsukuba Science City, Ibaraki 305, Japan.

M. D. Levine is with the Computer Vision and Robotics Laboratory, McGill Research Centre for Intelligent Machines, McGill University, Montreal, P.Q. H3A 2A7, Canada.

IEEE Log Number 8927496.

Index Terms—**Edge detection, image segmentation, range data analysis, region segmentation, surface curvature, 3-D object description.**

I. Introduction

In recent years, digital range data, referred to as a *range image* or *range* (*depth*) *map*, have become available for the analysis of three-dimensional (3-D) objects owing to the development of various active and passive range finding techniques [5], [11]. Conventional intensity images exhibit ambiguities in their interpretation as shapes of 3-D objects because of the complexities of object shape, reflectance and illumination. Range data provide direct geometrical information about the shape of visible surfaces so that some problems in 3-D object description and recognition should be solved more easily using range images rather than intensity images. In particular, an active range imaging system usually produces a dense range map which is useful for analyzing curved as well as polyhedral objects. Recently considerable attention has been paid to the problem of describing and a recognizing 3-D objects using range data [2].

The most significant problem in the early stages of image analysis is *image segmentation*, a process of partitioning an image into meaningful parts or extracting important image features from it. In general, image segmentation techniques are based on the common assumption that meaningful object components are homogeneous in image properties and that there exist abrupt changes in properties between the components. Segmentation techniques for range images can be classified into two categories: region- and edge-based approaches. A region-based approach, which is called *region segmentation*, attempts to group pixels into surface regions based on the homogeneity or similarity of surface properties. On the other hand, an edge-based approach, which is also referred to as *edge detection*, attempts to extract discontinuities in properties that form the closed boundaries of components.

Region-based methods for range images usually partition the image into surface regions which are approximately planar or quadric surfaces; see [9], [13], [15]. These approaches require the assumption that parts of object surfaces can be globally well approximated by a particular function. On the other hand, edge detection techniques in range images are intended to isolate discontinuities in both depth and surface orientation; for example, see [6], [18]. Edge-based approaches have been successful for analyzing polyhedral objects but have not been widely used for curved ones.

Besl and Jain [3] have proposed an attractive idea for surface characterization from the point of view of *differential geometry* [8], [12]. Smooth surfaces are locally characterized by a combination of the signs of Gaussian and mean curvatures, and are classified into one of eight surface types. However, there still remains a problem. Differential geometry is a theory for smooth differentiable surfaces, while the usual object surfaces are not entirely smooth but piecewise smooth. The problem is how the surface curvatures can be accurately calculated for piecewise smooth surfaces. Some of the solutions appearing in the literature are as follows: only shrunken surface regions are used as seeds for region growing [4]; surface curvatures are only computed for smooth areas after detecting jump discontinuities [19]; curvature-based classification is performed for segmented surface regions [20].

We propose a hybrid approach to the problem of range image segmentation, where "*hybrid*" refers to a combination of region- and edge-based considerations. The range image of an object is divided into surface primitives which are homogeneous in their intrinsic differential geometric properties and do not contain discontinuities in either depth or surface orientation. The method employs a selective surface fit and is based on the computation of first and second partial derivatives determined by locally approximating object surfaces using biquadratic polynomials. Then by computing the Gaussian and mean curvatures and examining their signs, an initial region-based segmentation is obtained in the form of a curvature sign map. Two initial edge-based segmentations are also computed from the partial derivatives and depth values. One detects jump edges by computing differences in depth, while the other highlights roof edges by differences in surface normals. The three initial image maps are then combined to produce the final range image segmentation.

The structure of this correspondence is as follows. In Section II, we first briefly discuss differential geometric properties of 3-D surfaces, especially the surface curvatures, and then show how to compute them for piecewise smooth surfaces. In Section III, our hybrid segmentation method is described in detail. We attempt to apply the method to synthetic and real range images in Section IV. Finally, Section V offers some conclusions.

II. Computing Differential Geometric Properties of Piecewise Smooth Surfaces

We first discuss the estimation of surface curvatures for describing 3-D object surfaces using differential geometry and then propose a technique for locally estimating them. It should be noted that differential geometry is a theory of smooth differentiable surfaces. However, objects are usually not entirely smooth over all their surfaces, but are piecewise smooth. The problem is how to accurately estimate curvature properties for piecewise smooth surfaces. The proposed selective local surface fit method is composed of three steps: 1) the selection of the best fit surface function to a local window centered at each point; 2) the determination of the best window orientation for each point; 3) the computation of surface curvatures from analytically calculated partial derivatives using the selected best window.

A. Surface Curvature and Range Data

Gaussian curvature is an intrinsic surface property which refers to an isometric invariant of a surface [8]. Both Gaussian and mean curvatures have the attractive characteristics of translational and rotational invariance. As pointed out by Besl and Jain [3], the signs of Gaussian and mean curvatures, denoted by K and H, respectively, yield a set of eight surface primitives. These possess desirable invariance properties including view-independency, and are powerful enough to describe visible surfaces. Given a coordinate system in which the z (depth) axis is directed toward the viewer, the eight surface primitives are: *peak*, *pit*, *ridge*, *valley*, *flat*, *minimal*, *saddle ridge*, and *saddle valley surfaces*. See [3] for detailed discussions as well as the pictorial shapes of these primitives.

It should be noted that the Gaussian and mean curvatures are local characteristics of a surface. This implies that they can be used for characterizing the surface in situations where occlusion is a problem. Thus we observe that it is attractive to use their signs as local surface shape descriptors for range image segmentation.

A depth surface is a range image observed from a single view can be represented by a digital graph (Monge patch) surface. That is, a depth or range value at a point (x, y) is given by a single-valued function $z(x, y)$. In this case, the Gaussian and mean curvatures are only related to the first and second partial derivatives of the function z with respect to x and y [8]. Thus the numerical computation of the surface curvature map only requires the first and second partial derivative estimates at each surface point.

B. Selective Local Surface Fit

We first determine the best fit function for the window centered at each point (x, y). Then for each (x, y) we choose the best window which provides a minimum fitting error among all the overlapping windows at that point.

1) Analytical Surface Fit: At each pixel in the range image, we locally determine a continuous differentiable function which fits the depth map surface. Note that what is being considered here is not a global fit but a local one. At least second order differentiability is needed for the function and it should be analytically simple. Surface fitting must not be sensitive to noise and quantization effects in the range images. Generally, we would expect higher order functions to fit the given data; however, this implies that such functions will not only approximate the local object shape but also the undesirable noise effects. These considerations lead us to choose the following biquadratic form which includes six independent parameters:

$$z(x, y) = ax^2 + by^2 + cxy + dx + ey + f. \tag{1}$$

We employ a local biquadratic surface fit within a $(2m + 1) \times (2m + 1)$ window centered at a point (x, y) and denoted by $W(x, y)$. We use a standard linear least squares method which was originally employed by Beaudet [1] for obtaining partial derivative estimators. The coefficients a–f can be obtained effectively by mask operators (see [22] for details). The coefficients are associated with a particular point (x, y) and therefore represented as $a(x, y)$, $b(x, y)$, $c(x, y)$, $d(x, y)$, and $f(x, y)$, respectively. The sum of the squared fitting error for the window $W(x, y)$ is referred to as $E^2(x, y)$:

$$E^2(x, y) = \sum_{i=-m}^{m} \sum_{j=-m}^{m} \{ai^2 + bj^2 + cij + di + ej + f - z(x + i, y + j)\}^2 \tag{2}$$

2) Selecting the Best Window: We recall that differential geometry is only useful for describing smooth differentiable surfaces, but unfortunately real objects are not entirely smooth. To accurately estimate the surface curvatures even in the vicinity of a discontinuity, the surface fit window for computing the partial derivatives must not overlap a discontinuity in the range data. We suggest a method for selecting the best window which does not overlap a discontinuity. For each point (x, y), we choose the best window $W(x - u, y - v)$ which provides a minimum fitting error among the covering $(2m + 1) \times (2m + 1)$ windows:

$$E^2(x - u, y - v) = \min \{E^2(k, l) : (k, l) \in W(x, y)\}. \tag{3}$$

This method is based on the fact that the surface fitting error increases in the neighborhood of a discontinuity. In practice, this selective surface fit is actually applied to only those points where E^2 is greater than a threshold.

Once the best window $W(x - u, y - v)$ has been determined, the surface fit at a point (x, y) is represented by a set of coefficients $\{a(x - u, y - v), b(x - u, y - v), c(x - u, y - v), d(x - u, y - v), e(x - u, y - v), f(x - u, y - v)\}$, where $(-u, -v)$ is a displacement from the point (x, y) to the center of the best window. The fitted depth value at the point (x, y) is then given by:

$$\begin{aligned} z(x, y) = {} & a(x - u, y - v)u^2 + b(x - u, y - v)v^2 \\ & + c(x - u, y - v)uv \\ & + d(x - u, y - v)u + e(x - u, y - v)v \\ & + f(x - u, y - v). \end{aligned} \tag{4}$$

We can also derive an *edge preserving smoothing* operator from (4). Such an operator is useful for smoothing range data corrupted by noise and quantization errors while preserving significant discontinuities [22].

This surface fit may be referred to as the *selective local surface fit*. While the idea behind the method comes from facet model smoothing of intensity images [10], this is the first application of the idea in range images. The basic approach is also similar to selective averaging [21], edge preserving smoothing [14], and computational molecules [7], [17].

C. Computing Partial Derivatives and Curvatures

Consider the computation of surface properties at an individual point in a range image. At the outset, the first and second partial derivatives are estimated based on the selective local surface fit. The surface curvatures are then calculated from the partial derivatives.

By using the selective local surface fit and symbolically differentiating (1), the first and second partial derivative estimates are obtained at a point (x, y) as follows:

$$\frac{\partial z}{\partial x}(x, y) = 2a(x-u, y-v)u + c(x-u, y-v)v + d(x-u, y-v) \quad (5)$$

$$\frac{\partial z}{\partial y}(x, y) = 2b(x-u, y-v)v + c(x-u, y-v)u + e(x-u, y-v) \quad (6)$$

$$\frac{\partial^2 z}{\partial x^2}(x, y) = 2a(x-u, y-v) \quad (7)$$

$$\frac{\partial^2 z}{\partial y^2}(x, y) = 2b(x-u, y-v) \quad (8)$$

$$\frac{\partial^2 z}{\partial x \partial y}(x, y) = \frac{\partial^2 z}{\partial y \partial x}(x, y) = c(x-u, y-v). \quad (9)$$

Substituting the mask operators (see [22] for details) for the coefficients into (5)–(9), we obtain a set of the partial derivative estimators which include the displacement (offset) $(-u, -v)$. A set of 5×5 finite difference operators are shown in the Appendix. Note that the operators with no displacements are equivalent to the second order operators proposed by Beaudet [1].

The Gaussian and mean curvatures are computed using the partial derivatives given above. Fig. 1 shows that the selective local surface fit method improves the curvature estimates when compared to the fixed nonadaptive window method. It can be observed that surface points are correctly characterized by using the proposed surface fit technique even in the neighborhood of discontinuities.

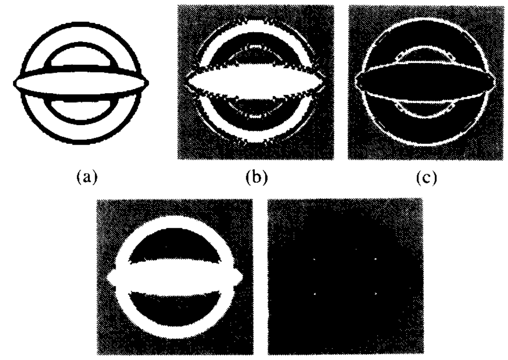

Fig. 1. Comparison of the selective local surface fit with the conventional nonadaptive window method for computing curvature sign maps. In this figure, the Gaussian and mean curvature sign maps are pesented for a synthetic range image which contains an ellipsoid and a partially occluded torus. Positive curvature is shown in white, zero curvature in gray, and negative curvature in black. The selective local surface fit was performed at the points whose error of fits E^2 was greater than a certain thresholds (0.1). Other thresholds needed to produce the sign maps were set equally for both methods. The window size used was 5×5. (a) shaded image; (b) Gaussian and (c) mean curvature sign maps using the nonadaptive method; (d) Gaussian and (e) mean curvature sign maps using the selective local surface fit.

IV. Hybrid Approach to Range Image Segmentation

A. *What Is Meant by Range Image Segmentation?*

We wish to partition a range image into meaningful surface regions without using any domain-specific knowledge. The problem to be discussed here is how to define a domain-independent segmentation of range data; in other words, what is a meaningful surface region in the range data? Special types of objects and their shapes are not assumed. A scene may be composed of several objects and there may be occlusions. The only assumption used here is that an object surface is partially composed of smooth differentiable surfaces.

Considering the above, the surface region is defined to be the largest four-connected component which satisfies the following two conditions:

1) The surface area is homogeneous in its view-independent differential geometric properties; in other words, the signs of the Gaussian and mean curvatures are constant within the area.

2) The area does not contain any significant discontinuities in either depth or surface orientation.

The first condition is not sufficient for the definition of the surface region, since distinct surfaces having the same combination of curvature signs may appear to be adjacent to each other. This case can easily occur in a range image; for example, two planar surfaces meet at a straight line in a polyhedral object where they share a roof edge; two distinct surfaces of the same surface type may share a jump edge at an occluding contour. This supports the necessity for integrating edge information into a region-based scheme for range image segmentation.

B. *Description of the Approach*

Here we present an overview of our approach to range image segmentation. The computational flow consists of the following three major steps:

1) Local Surface Characterization: The first and second partial derivatives are first estimated at each surface point. These should be accurately computed not only as a smooth surface but also in the neighborhood of a discontinuity using the selective local surface fit. By using these partial derivatives, the surface normal and surface curvatures can be calculated.

2) Initial Segmentation: Three kinds of initial segmentation are computed in parallel: a region-based segmentation in the form of a curvature sign map (KH-sign map) and two edge-based segmentations embodying the jump and roof edge maps.

3) Final Segmentation: The three initial segmentation maps are combined to produce the final segmentation in which each region must satisfy the surface region conditions mentioned earlier. Since the first step has been described earlier, the following discussion focusses on the initial and final segmentation stages.

C. *Region-Based Initial Segmentation: Curvature Sign Map*

The initial region-based segmentation is equivalent to the method of Besl and Jain [3], except for the use of the selective local surface fit. Theoretically surface points can be classified into one of eight surface primitives according to the signs of K and H. However, in practice thresholding about zero is required to obtain the curvature sign map. For example, the range image of a flat surface does not yield Gaussian and mean curvature values which are exactly equal to zero. This is usually caused by noisy variations in depth and quantization effects. We select thresholds which are symmetric about zero for the Gaussian and mean curvatures; these are referred to as K_{zero} and H_{zero}, respectively.

The selection of K_{zero} and H_{zero} poses a problem. We note that the following constraint is available:

$$K_{zero} \geq H_{zero}^2. \quad (10)$$

This condition comes from the fact that if (10) is not satisfied, some surface points may fall into a prohibitive zone in (K, H) space where $K > 0$ and $H = 0$. Besl and Jain have suggested a method for setting these parameters in which the maxima of both curvatures are employed as criteria [3]. However, the optimal values of these thresholds are generally thought to depend on the noise level in the range images. It can reasonably be argued that the noise variations are caused by the range finder and the calibration process and is not dependent upon the underlying objects.[1] If we assume that these

[1]We are indebted to Gerhard Roth at the McGill Research Centre for Intelligent Machines for this suggestion.

two factors are fixed, a systematic approach to threshold selection can be proposed as follows: 1) compute K and H for a *reference flat surface* obtained by the scanner; 2) set K_{zero} and H_{zero} to the minimum values necessary to classify the surface as flat while satisfying the constraint of (10).

Small surface regions regarded as noise may be present, and to erase these the KH-sign map is contracted and then expanded. First each surface region in the map is contracted by one pixel, considering four-connectedness for pixel connectivity. The surface region is then iteratively expanded until all unlabeled pixels are eliminated. Existing contraction and expansion operators for binary images can be used. The resulting map is referred to as a refined KH-sign map.

D. Edge-Based Initial Segmentation

In this section we briefly mention the detection of discontinuities in depth and surface orientation.

1) Detecting Depth Discontinuity: Jump Edge Map: The jump edge magnitude, denoted by M_{jump}, is computed as the maximum difference in depth between a point and its eight neighbors. This is formulated for a point (x, y) as follows:

$$M_{jump}(x, y) = \max \left\{ \left| z(x, y) - z(x + k, y + l) \right| : -1 \le k, l \le 1 \right\} \quad (11)$$

where z represents a value of the fitted polynomial computed from (4). The edge image is thresholded for the final segmentation. At present the threshold is automatically determined based on the mean and standard deviation of the edge magnitude.

2) Detecting Surface Orientation Discontinuity: Roof Edge Map: A roof edge can be located by surface normal analysis. The roof edge magnitude, denoted by M_{roof}, is computed as the maximum angular difference between adjacent unit surface normals. This is formally given as:

$$M_{roof}(x, y) = \max \left\{ \cos^{-1} \left(\mathbf{n}(x, y) \cdot \mathbf{n}(x + k, y + l) \right) : -1 \le k, l \le 1 \right\} \quad (12)$$

where $\mathbf{n}$ denotes a unit surface normal obtained from estimates of the first partial derivative. This must also be thresholded to combine it with the KH-sign and jump edge map at the final segmentation stage.

Recall in the previous section that the discontinuities in the range image were roughly estimated by using the surface fit error for selecting the best window at each point. The surface fit error highlights the discontinuities but cannot discriminate jump and roof discontinuities. The discrimination of these edge types is thought to be important for later object analysis. It is for this reason that we employ different operators for locating these discontinuities.

E. Final Segmentation

We present a method for integrating the three initial segmentation maps to produce the final segmentation. The method is composed of the following three steps: 1) superimposing the edge maps onto the KH-sign map; 2) component analysis of surface regions; 3) expansion of surface regions.

1) Superimposing Edge Maps onto the KH-Sign Map: After the initial region-based segmentation, the KH-sign map exists in the form of a labeled image in which each point has a value from the set 1 to 8 corresponding to the determined surface type. At this stage the thresholded edge maps are superimposed onto the KH-sign map to produce a *surface-edge map*, in which each edge point has a value of -2 or -1 if it is regarded as a jump or roof edge, respectively. In other words, the surface-edge map is composed of surface points having positive values and edge points having negative values.

2) Component Analysis: To generate a region map, an existing four-connected component labeling algorithm is independently employed for each surface type in the *surface-edge map*. The edge points are not labeled and are kept unchanged. Thus the resulting region map is not a complete segmentation; i.e., it is composed of surface points which possess region numbers as their labels and edge points with negative labels.

3) Expansion of Surface Regions: Each surface region in the previously obtained partial region map is expanded in parallel to generate a final region map using the following two steps. First, each surface region having a positive label is conditionally expanded so that the expansion does not cross the boundaries of surface regions in the refined KH-sign map. However, there still remain edge points with negative labels which correspond to the surface points entirely overlapped by edge points. Each surface region is then unconditionally expanded in parallel until all edge points are erased.

Simultaneously, to produce the final surface type map corresponding to the above region map, each surface region in the *surface-edge* map is expanded in the same manner as described above. As a consequence, surface regions entirely overlapped by edge points are not recovered; i.e., small surface regions on discontinuities are thereby eliminated.

IV. Experimental Results

We have obtained experimental results for the proposed segmentation method using both synthetic and real range data. In the results shown here, the first and second partial derivatives were computed using 5 × 5 operators.

A. Synthetic Range Data

We first present the results for synthetic data. These are represented in the form of a 2-D array consisting of floating point numbers which indicate the depth values relative to a background and do not suffer from either noise or quantization effects.

Fig. 2 shows the boundary representations for the final region and surface type maps for the synthetic data in Fig. 1. The thresholds about zero for K and H were selected as $K_{zero} = 0.00001$ and $H_{zero} = 0.003$, respectively. The jump and roof edge maps were thresholded using the values of mean plus standard deviation of their magnitudes. It can be seen that the horizontal ellipsoid and the outside surface of the torus are discriminated in the region map, while these are merged in the surface type map because of their characteristics as peak surfaces. Thus distinct adjacent surface regions of the same surface type are isolated by employing edge information.

B. Real Range Data

Real range images used in the experiments were obtained using a laser range scanner [16]. The images were originally provided as a 2-D array of pixels with values 12 bits long and proportional to the z values. These were then calibrated, resulting in floating point data. These range images do not suffer as much from quantization effects when compared to the typical 8 bit images reported in the literature. However, they do contain some shadow effects. Although the image size is 256 × 256, in order to limit the computation time experiments were carried out with 128 × 128 images obtained by resampling.

Experimental results for real data are illustrated in Fig. 3. The scene consists of both curved and polyhedral objects. Spherical and cylindrical objects which are partially occluded can be seen in the image. In this case, edge preserving smoothing was applied twice to the range image before the computation of the partial derivatives. By noting the values of K and H in the background (regarded as a flat surface), the thresholds K_{zero} and H_{zero} were manually set to 0.0004 and 0.02, respectively. Jump and roof edge maps were thresholded by the mean of the edge magnitude. Fairly good results were obtained for extracting and describing the surfaces of spherical, cylindrical and polyhedral objects. Note that the polyhedral objects are excellently partitioned into their planar surfaces due to the integration of the edges with curvature sign map. However, a

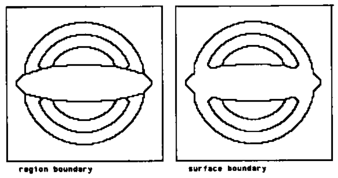

(a) (b)

Fig. 2. Experimental results for synthetic data: (a) region map; (b) surface type map.

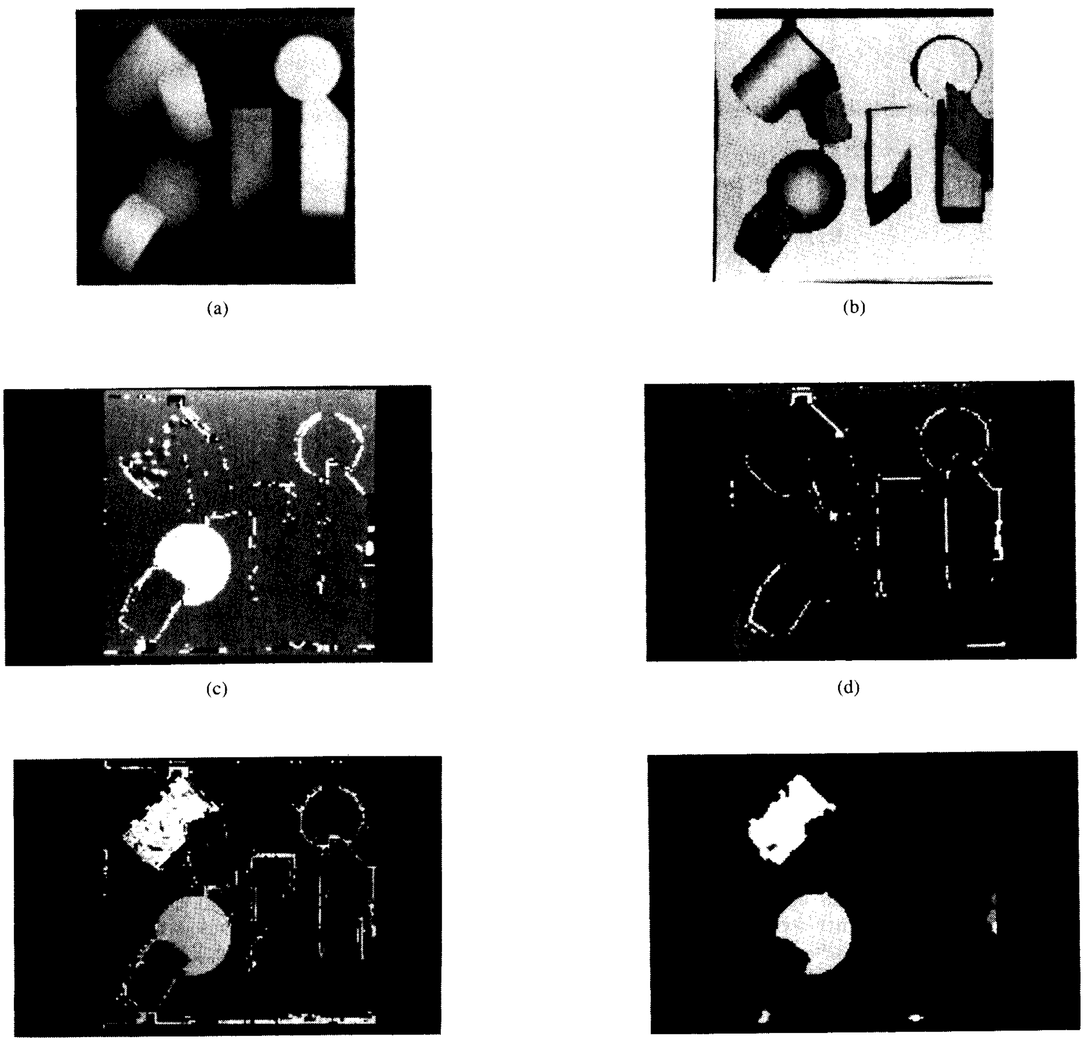

(a) (b) (c) (d) (e) (f)

Fig. 3. Experimental results for a real range image: (a) range image; (b) shaded image; (c) Gaussian curvature sign map; (d) mean curvature sign map (e) KH-sign map; (f) refined KH-sign map.

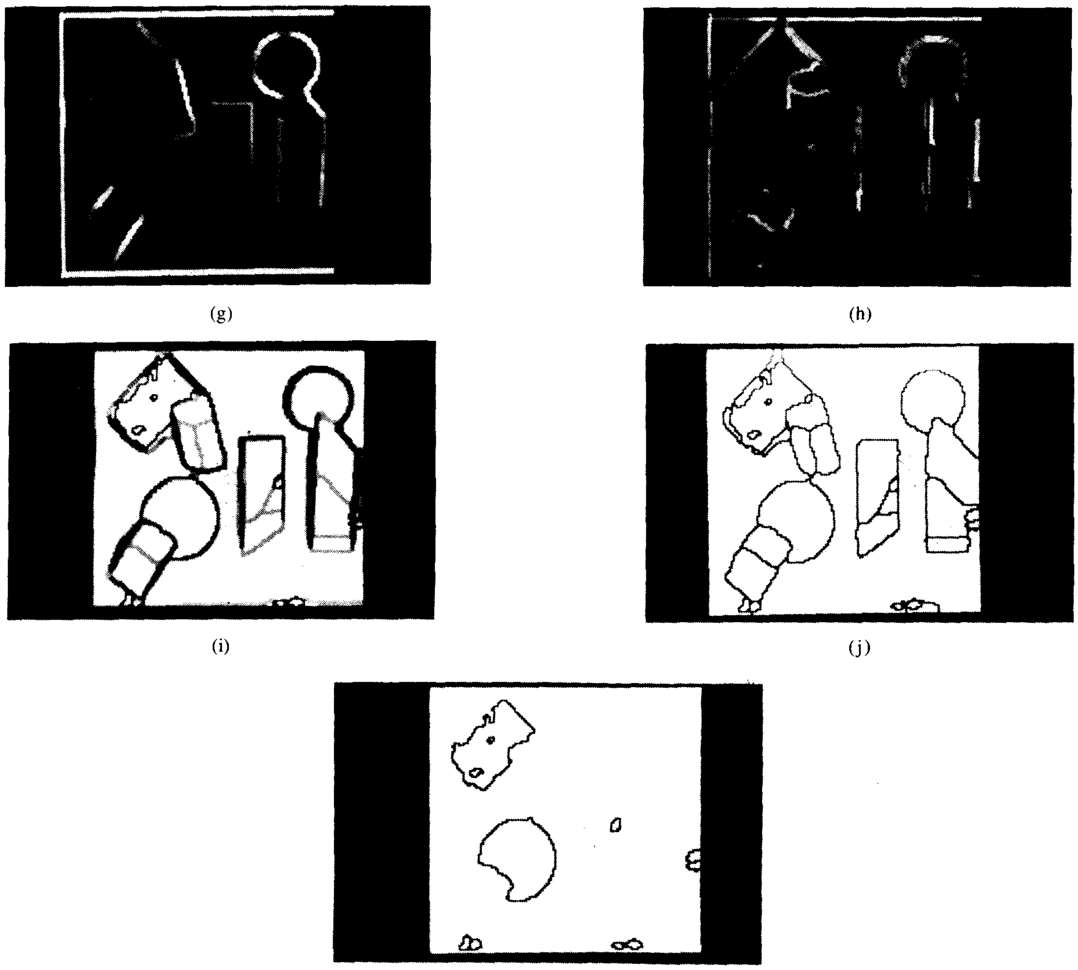

Fig. 3. (*Continued.*) (g) Jump edge map; (h) roof edge map; (i) surface-edge map; (j) region map; (k) surface type map.

few small surface regions appear at the corner of planar surfaces and in the vicinity of image borders. These are created by the impossibility of selecting windows which do not overlap any discontinuities; that is, all possible windows overlap discontinuities.

V. Conclusions

In this correspondence, we have proposed a hybrid approach to range image segmentation. We first locally approximate a depth surface using a selective surface fit and analytically compute the partial derivatives. The Gaussian and mean curvatures and the surface normal are then computed at individual points. By using these quantities, three kinds of initial segmentation maps are generated in parallel: 1) KH-sign map; 2) jump edge map; 3) roof edge map. Finally, these maps are combined into the final segmentation.

The usefulness of this approach has been proven experimentally for both synthetic and real range data containing polyhedral and curved objects. The contributions of this paper are summarized as follows:

1) Surface points are accurately characterized as one of eight possible view-independent surface types, even in the vicinity of discontinuities in depth and surface orientation. This is accomplished by the use of the proposed local surface fit technique.

2) Adjacent distinct surface regions of the same surface type can be discriminated. This advantage is due to the integration of edge information into a region-based segmentation scheme.

3) In addition to segmented region maps, rich descriptions of the surface and boundary of a region are obtained [22]. These are thought to be useful for further object recognition. Major problems that remain can be stated as follows:

1) The thresholds K_{zero} and H_{zero} for the Gaussian and mean curvature sign maps were selected manually. Different values of the thresholds yield different KH-sign maps, and subsequently different region maps. The threshold selection technique should be investigated further.

2) The proposed selective local surface fit will usually accurately estimate surface curvatures in the neighborhood of discontinuities. However, as can been seen in the experimental results sometimes all possible windows overlap discontinuities and wrong curvature estimates are subsequently obtained. A possible solution to this problem is to use a variable window size (multiscale approach) or variable window shape (e.g., [14]).

The present work provides an input to the 3-D object recognition process. Our segmentation method yields a rich description of a scene in terms of its surface primitives. Local and global properties, for example the surface type, edge type and surface area are part of this description. Such features are then used as matching primitives for 3-D object recognition. In particular, view-independent characteristics of surfaces, together with region-based descriptions, are quite useful for recognizing curved as well as polyhedral objects.

Appendix

A set of 5×5 operators for estimating the first and second partial derivatives using the selective local surface fit is given below.

$$\frac{\partial z}{\partial x} : \frac{1}{700} \begin{bmatrix} 40u - 28v - 28 & -20u - 14v - 14 & -40u & -20u + 14v + 14 \\ 40u - 14v - 28 & -20u - 7v - 14 & -40u & -20u + 7v + 14 \\ 40u - 28 & -20u - 14 & -40u & -20u + 14 \\ 40u + 14v - 28 & -20u + 7v - 14 & -40u & -20u - 7v + 14 \\ 40u + 28v - 28 & -20u + 14v - 14 & -40u & -20u - 14v + 14 \end{bmatrix} \begin{bmatrix} 40u + 28v + 28 \\ 40u + 14v + 28 \\ 40u + 28 \\ 40u - 14v + 28 \\ 40u - 28v + 28 \end{bmatrix}$$

$$\frac{\partial z}{\partial y} : \frac{1}{700} \begin{bmatrix} -28u + 40v + 28 & -14u + 40v + 28 & 40v + 28 & 14v + 40v + 28 \\ -14u - 20v + 14 & -7u - 20v + 14 & -20v + 14 & 7u - 20v + 14 \\ -40v & -40v & -40v & -40v \\ 14u - 20v - 14 & 7u - 20v - 14 & -20v - 14 & -7u - 20v - 14 \\ 28u + 40v - 28 & 14u + 40v - 28 & 40v - 28 & -14u + 40v - 28 \end{bmatrix} \begin{bmatrix} 28u + 40v + 28 \\ 14u - 20v + 14 \\ -40v \\ -14u - 20v - 14 \\ -28u + 40v - 28 \end{bmatrix}$$

$$\frac{\partial^2 z}{\partial x^2} : \frac{1}{35} \begin{bmatrix} 2 & -1 & -2 & -1 & 2 \\ 2 & -1 & -2 & -1 & 2 \\ 2 & -1 & -2 & -1 & 2 \\ 2 & -1 & -2 & -1 & 2 \\ 2 & -1 & -2 & -1 & 2 \end{bmatrix} \qquad \frac{\partial^2 z}{\partial y^2} : \frac{1}{35} \begin{bmatrix} 2 & 2 & 2 & 2 & 2 \\ -1 & -1 & -1 & -1 & -1 \\ -2 & -2 & -2 & -2 & -2 \\ -1 & -1 & -1 & -1 & -1 \\ 2 & 2 & 2 & 2 & 2 \end{bmatrix}$$

$$\frac{\partial^2 z}{\partial x \partial y}, \frac{\partial^2 z}{\partial y \partial x} : \frac{1}{100} \begin{bmatrix} -4 & -2 & 0 & 2 & 4 \\ -2 & -1 & 0 & 1 & 2 \\ 0 & 0 & 0 & 0 & 0 \\ 2 & 1 & 0 & -1 & -2 \\ 4 & 2 & 0 & -2 & -4 \end{bmatrix}$$

Acknowledgment

The authors wish to acknowledge the assistance of the National Research Council of Canada for providing us with laser range images. They also would like to thank B. I. Demir and D. Gauthier for their helpful discussions and assistance in developing programs for this work. N. Yokoya would like to thank the Science and Technology Agency of Japan for its support during his study leave. M. D. Levine would like to thank the Canadian Institute for Advanced Research for its support.

References

[1] P. R. Beaudet, "Rotationally invariant image operators," in *Proc. 4th Int. Joint. Conf. Pattern Recognition*, Kyoto, Nov. 1978, pp. 579–583.

[2] P. J. Besl and R. C. Jain, "Three-dimensional object recognition," *ACM Comput. Surveys*, vol. 17, pp. 75–145, Mar. 1985.

[3] P. J. Besl and R. C. Jain, "Invariant surface characteristics for 3D object recognition in range images," *Comput. Vision, Graphics, Image Processing*, vol. 33, pp. 33–80, Jan. 1986.

[4] —, "Segmentation through symbolic surface descriptions," in *Proc. IEEE Conf. Computer Vision and Pattern Recognition*, June 1986, pp. 77–85.

[5] P. J. Besl, "Range image sensors," Dep. Comput. Sci., General Motors Res. Labs., Warren, MI, Rep. GMR-6090, Mar. 8, 1988.

[6] B. Bhanu, S. Lee, C. C. Ho, and T. Henderson, "Range data processing: Representation of surfaces by edges," in *Proc. 8th Int. Conf. Pattern Recognition*, Oct. 1986, pp. 236–238.

[7] M. Brady, J. Ponce, A. Yuille, and H. Asada, "Describing surfaces," *Comput. Vision, Graphics, Image Processing*, vol. 32, pp. 1-28, Oct. 1985.

[8] M. P. do Carmo, *Differential Geometry of Curves and Surfaces*. Englewood Cliffs, NJ: Prentice-Hall, 1976.

[9] O. D. Faugeras, M. Hebert, and E. Pauchon, "Segmentation of range data into planar and quadratic patches," in *Proc. IEEE Conf. Computer Vision and Pattern Recognition*, June 1983, pp. 8–13.

[10] R. M. Haralick and L. Watson, "A facet model for image data," *Comput. Graphics Image Processing*, vol. 15, pp. 113–129, Feb. 1981.

[11] R. A. Jarvis, "A perspective on range finding techniques for computer vision," *IEEE Trans. Pattern Anal. Machine Intell.*, vol. PAMI-5, pp. 122–139, Mar. 1983.

[12] M. M. Lipschutz, *Theory and Problems of Differential Geometry*. New York: McGraw-Hill, 1969.

[13] Y. Muller and P. Mohr, "Planes and quadrics detection using Hough transform," in *Proc. 7th Int. Conf. Pattern Recognition*, Aug. 1984, pp. 1101–1103.

[14] M. Nagao and T. Matsuyama, "Edge preserving smoothing," *Comput. Graphics Image Processing*, vol. 9, pp. 394–407, Apr. 1979.

[15] M. Oshima and Y. Shirai, "Object recognition using three-dimensional information," *IEEE Trans. Pattern Anal. Machine Intell.*, vol. PAMI-5, pp. 353–361, July 1983.

[16] M. Rioux, "Laser range finder based on synchronized scanners," *Appl. Opt.*, vol. 23, pp. 3837–3844, Nov. 1984.

[17] D. Terzopoulos, "The role of constraints and discontinuities in visible-surface reconstruction," in *Proc. 8th Int. Joint Conf. Artificial Intelligence*, Aug. 1983, pp. 1073–1077.

[18] F. Tomita and T. Kanade, "A 3D vision system: Generating and matching shape descriptions in range images," in *Proc. 1st Conf. Artificial Intelligence Applications*, Dec. 1984, pp. 186–191.

[19] B. C. Vemuri, A. Mitiche, and J. K. Aggarwal, "Curvature-based representation of objects from range data," *Image Vision Comput.*, vol. 4, pp. 107–114, May 1986.

[20] H. S. Yang and A. C. Kak, "Determination of the identity, position and orientation of the topmost object in a pile," *Comput. Vision, Graphics, Image Processing*, vol. 36, pp. 229–255, Nov./Dec. 1986.

[21] N. Yokoya, T. Kitahashi, K. Tanaka, and T. Asano, "Image segmentation scheme based on a concept of relative similarity," in *Proc. 4th Int. Joint Conf. Pattern Recognition*, Kyoto, Japan, Nov. 1978, pp. 645–647.

[22] N. Yokoya and M. D. Levine, "Range image segmentation based on differential geometry: A hybrid approach," McGill Research Centre for Intelligent Machines, McGill University, Montreal, P.Q., Canada, Rep. McRCIM-TR-CIM 87-16, 1987.